

Temperature and Intensity Dependence of Intersubband Relaxation Rates from Photovoltage and Absorption

J. N. Heyman

Department of Physics and Astronomy, Macalester College, St. Paul, Minnesota 55105

K. Unterrainer, K. Craig, B. Galdrikian, and M. S. Sherwin

Department of Physics and Center for Free Electron Laser Studies, University of California at Santa Barbara, Santa Barbara, California 93106

K. Campman, P. F. Hopkins, and A. C. Gossard

Materials Department, University of California at Santa Barbara, Santa Barbara, California 93106

(Received 22 August 1994)

We report intersubband-scattering times (T_1) in a semiconductor heterostructure with intersubband spacing below the LO phonon energy. T_1 is determined by simultaneous measurements of the intersubband absorption and the photovoltage induced by far-infrared radiation (FIR) near the intersubband transition frequency. At the lowest temperature ($T = 10$ K) and FIR intensity ($I = 10$ mW/cm²), $T_1 = 1.2 \pm 0.4$ ns, several times longer than predicted theoretically. T_1 decreases strongly with increasing temperature and FIR intensity, to 20 ps at $T = 50$ K in the linear regime, and to 15 ps at $T = 10$ K and $I = 2$ kW/cm².

PACS numbers: 42.65.Ky, 73.20.Dx, 78.55.-m

Intersubband transitions of electrons in quantum wells can be used to engineer infrared detectors and nonlinear optical devices. The recent development of a mid-infrared intersubband laser [1] has renewed interest in the development of an intersubband laser operating in the far infrared. A critical parameter for such devices is the nonradiative intersubband relaxation time (T_1). In quantum wells in which the subband spacing is less than the optical-phonon energy, energy relaxation can proceed by acoustic phonon scattering, by electron-electron and electron-impurity scattering, and (at nonzero temperature) by optical phonon scattering, but the relative importance of these processes is not understood. Theoretical estimates [2] of intersubband lifetimes in wide quantum wells in which $E_{1,2} < \hbar\Omega_{LO}$ are of the order of hundreds of picoseconds. Time-resolved [3–5] and steady-state [6–8] measurements using a variety of experimental techniques have been performed, yielding values of T_1 that vary over several orders of magnitude. Murdin *et al.* [5] report $T_1 = 40 \pm 5$ ps in a 270 Å square well using time-resolved measurements of the intersubband absorption; Craig *et al.* [7] deduce T_1 of order 1 ns using saturated-absorption measurements; Li *et al.* [6] report $T_1 \approx 1.2$ ns for coupled intersubband Landau transitions in a double-well structure; and Faist *et al.* [8] obtain a relaxation time of $T_1 = 300 \pm 100$ ps in a double-well structure using a steady-state, differential-absorption technique.

In this Letter, we measure T_1 in a coupled-well structure with $E_{1,2} < \hbar\Omega_{LO}$ by measuring the *photovoltage and the intensity-dependent absorption* associated with the intersubband transition. The photovoltage we measure is due to the transfer of electrons from the ground to the excited subbands of the well, and is proportional to the

population in the excited state. A similar effect has been observed previously in step quantum wells [9,10]. The strength of the combined measurement of photovoltage and absorption is that the relaxation time can be measured as a function of both excitation intensity and temperature. Thus we can study both the low-temperature, linear-response regime important for devices like detectors and mixers and the hotter, strongly excited environments likely to be encountered in lasers. We obtain relaxation times that vary by several orders of magnitude but correlate with sample condition, temperature, and pump light intensity.

The heterostructure was grown by molecular beam epitaxy on a semi-insulating substrate. It consists of 4500 Å of a 20 Å superlattice (14 Å GaAs, 6 Å AlAs); a doping region (520 Å Al_{0.3}Ga_{0.7}As with 26 Si delta-doped layers giving a total charge concentration of 1.2×10^{12} cm⁻²); 700 Å of the superlattice; a 73 Å GaAs well; a 25 Å Al_{0.3}Ga_{0.7}As barrier, an 85 Å GaAs well; a spacer layer, doping region, and barrier region identical to the above; and a 50 Å GaAs capping layer [11]. The lowest electron-subband spacing was measured to be $E_2 - E_1 = 11$ meV using photoluminescence with no applied bias. Energies of the higher subbands $E_3 - E_1 = 110$ meV and $E_4 - E_1 = 156$ meV were obtained from a self-consistent model described below. The measurements described in this work were performed near resonance with $h\nu \approx E_2 - E_1$. Under these conditions the heterostructure may be approximated as a two-subband system. At low temperatures ($T < 50$ K), the zero-bias charge density measured by Hall effect is $N_s = 2 \times 10^{11}$ cm⁻², and the electron in-plane mobility is $\mu = 1 \times 10^5$ cm²/V s.

A Schottky gate was evaporated on the surface of the structure, and Ohmic contacts were made to the double

well. A negative voltage between the gate and Ohmic contacts imposes a dc electric field across the structure and depletes it of charge. Measurements of capacitance versus gate voltage [$C(V_g)$] determine that the well is fully depleted at -1.6 V bias ($E = 15$ kV/cm). Aluminum was also evaporated on the substrate side of the wafer, so that the sample formed a parallel-plate waveguide. In these experiments, far-infrared polarized (FIR) radiation is coupled into the cleaved edge of the wafer with E parallel to the growth direction.

FIR linear-absorption and resonant harmonic-generation measurements on this structure have been reported elsewhere [11,12]. The absorption spectrum between 5 and 200 cm^{-1} consists of a single line whose position can be tuned between 14.5 and 10 meV with gate bias. At -0.8 V bias the peak position is $\hbar\tilde{\omega}_{1,2} = 12.8$ meV (103 cm^{-1}) and the line shape is approximately Lorentzian with a full width at half maximum of 0.82 meV. There is a difference between the energy of the absorption resonance and the bare subband spacing (we calculate $\hbar\tilde{\omega}_{1,2} = 10.25$ meV at -0.8 V bias) due to the depolarization shift [13].

Our photovoltage experiments employ the UCSB Free-Electron Laser (FEL) as a far-infrared pump. The laser produces 5 μs pulses of 103 cm^{-1} radiation at a 1.5 Hz repetition rate. The FIR uniformly illuminates the edge of our sample, which is mounted in a variable-temperature cryostat. The photovoltage is observed as a laser-induced voltage between the gate and the quantum well, and arises because the expectation value of the position of an electron in an excited state and the ground state are different. Radiation transmitted through the sample is focused onto a 4.2 K Ge bolometer, so that intersubband absorption and light-induced polarization can be measured simultaneously. We investigate resonant effects by tuning the intersubband absorption resonance through the laser frequency with gate bias.

The time structure of the photovoltage and the FIR laser pulse are the same within the 300 kHz bandwidth of our preamplifier. Figure 1(a) shows the amplitude of the photovoltage and the FIR transmission as a function of gate bias, measured at $T = 10$ K, and a laser intensity of 0.32 W/cm^2 . A resonance in the photovoltage occurs when the intersubband-absorption frequency is tuned through the laser frequency at $V_G = -0.8$ V, indicating that the photovoltage is associated with the intersubband transition.

Figure 2(a) shows the temperature dependence of the sensitivity of the photovoltage (the photovoltage at resonance divided by laser intensity) and the intersubband absorption coefficient measured at resonance. These measurements were made at low intensities, where the sensitivity is independent of the laser intensity. While the absorption coefficient decreases by a factor of 2.3 between 10 and 70 K, the photovoltage sensitivity decreases by a factor of 10^4 between 10 and 160 K. At temperatures $T \leq 50$ K, the line shapes of the absorption and

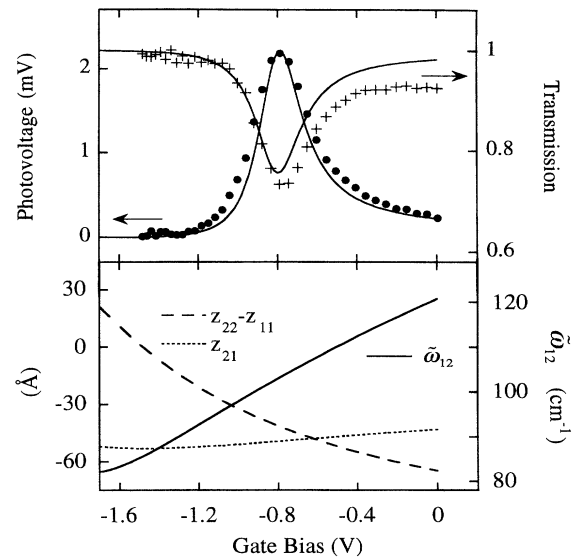


FIG. 1. (a) Photovoltage and transmission in our asymmetric coupled-well sample in the linear regime ($T = 10$ K, $I = 0.32$ W/cm^2). Gate bias is used to tune the intersubband absorption resonance through the FIR laser frequency ($\hbar\nu = 103$ cm^{-1}). Solid lines are calculated from theory (see text). (b) Calculated resonance frequency and dipole matrix elements for our structure as a function of gate bias, obtained from our self-consistent model.

photovoltage are nearly constant. At higher temperatures, the absorption line shape varies weakly with temperature. On the other hand, the photovoltage line shape changes significantly at $T > 50$ K, becoming strongly asymmetric and changing sign near $V = -0.8$ V.

Figure 3(a) shows the sensitivity (photovoltage/intensity) and the intersubband absorption at resonance as a function of pump intensity at $T = 10$ K. Both the sensitivity and the absorption coefficient are constant at low intensities. The sensitivity decreases by 50% at an intensity $I \approx 1$ W/cm^2 , while the absorption coefficient decreases by 50% only at $I \approx 200$ W/cm^2 .

To describe our results, we calculated the energies and envelope functions of electrons at the subband minima in our double well by self-consistently solving the Schrödinger and Poisson equations within the effective-mass approximation. Temperature effects were included by allowing thermal population of higher subbands.

We model the absorption and photovoltage in our well using perturbation theory. The linear absorption cross section $\sigma(\omega)$ of an electron in a two-subband quantum well is given (in CGS units) by

$$\sigma(\omega) = \frac{4\pi\omega e^2 |z_{1,2}|^2}{c\sqrt{\epsilon} \hbar [(\omega - \tilde{\omega}_{1,2})^2 + T_2^{-2}] T_2}. \quad (1)$$

Here, $z_{i,j}$ is the dipole-matrix operator between states i and j , $\tilde{\omega}_{1,2}$ is the depolarization-shifted intersubband-absorption resonance frequency, and T_2 is the dephasing time. In our coupling geometry, the intensity-dependent

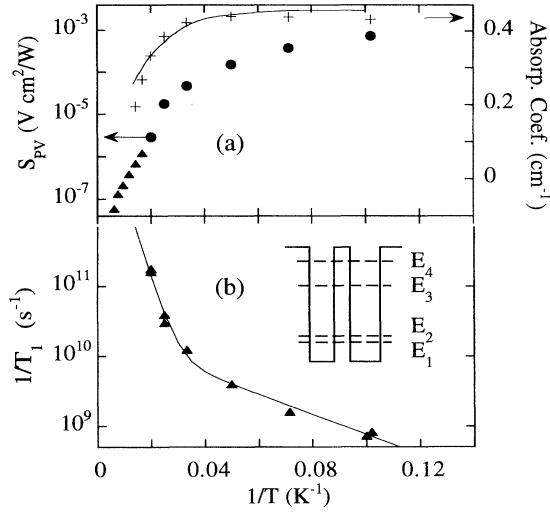


FIG. 2. (a) S_{pv} (photovoltage divided by laser intensity) and intersubband absorption coefficient versus inverse temperature, measured at low pump intensities. The solid line is the calculated absorption coefficient. We do not fully understand the photovoltage response at $T > 50$ K (\bullet), although the trend of the data agrees with our model. (b) The intersubband-scattering rate calculated from these data is strongly temperature dependent. The solid line is a fit to the data (see text). Inset is a sketch of the conduction band of our device. Transitions occur between E_1 and E_2 .

absorption coefficient is

$$\alpha(I) = (\Delta n_{1,2}^0) \frac{\sigma}{a} \left(1 + 2 \frac{I\sigma T_1}{\hbar\omega}\right)^{-1}, \quad (2)$$

where $\Delta n_{1,2}^0$ is the difference between the equilibrium populations of the first and second subbands, I is the intensity of the pump beam, T_1 is the intersubband relaxation time, and a is the thickness of the sample

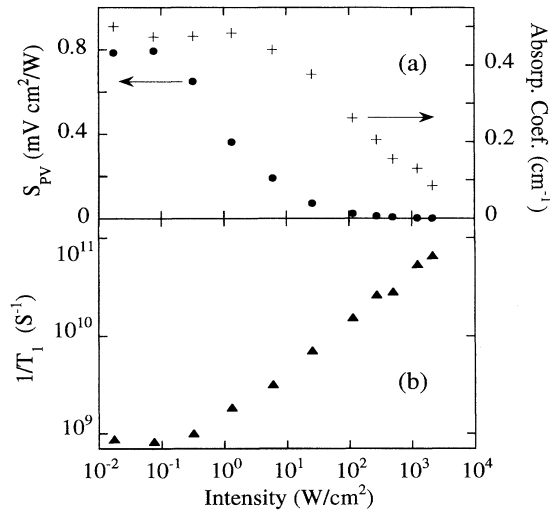


FIG. 3. (a) S_{pv} (photovoltage divided by intensity) and intersubband absorption coefficient versus pump intensity measured at $T = 10$ K. (b) The intersubband-scattering rate calculated from this data depends strongly on intensity.

(500 μm). The optically induced polarization P in our well under steady excitation is given by

$$P = -e(z_{2,2} - z_{1,1}) (\Delta n_{1,2}^0) \frac{I\sigma T_1}{\hbar\omega} \left(1 + 2 \frac{I\sigma T_1}{\hbar\omega}\right)^{-1}. \quad (3)$$

We calculated subband energies, dipole matrix elements, and the depolarization shift at each gate bias from our simulation. The calculated and measured [Fourier transform infrared (FTIR) absorption] absorption frequencies agree. We obtained the dephasing time versus gate bias from the linewidth of the intersubband absorption (measured with FTIR). With these data, our model allows us to calculate the FIR transmission and photovoltage $\Delta V = 4\pi P/\epsilon$ of our sample at low intensity (Fig. 1, solid lines). The calculated values of $\tilde{\omega}_{12}$, z_{12} , and $z_{11} - z_{22}$ as a function of gate bias are given in Fig. 1(b). At resonance (gate voltage $V_g = -0.8$ V), the calculated dipole matrix elements are $z_{12} = 49$ \AA and $z_{22} - z_{11} = 41.7$ \AA , the carrier concentration is $N_s = 1.8 \times 10^{11} \text{ cm}^{-2}$, and the Fermi level is 4.2 meV above the first subband. At $V_g = -1.3$ V the levels in the coupled well go through an anticrossing, and $z_{11} - z_{22}$ changes sign. This anticrossing is observed experimentally as a change in the sign of the photovoltage near $V = -1.3$ V.

Fitting the magnitude of the photovoltage to experiment yields an intersubband lifetime $T_1 = 1.2 \pm 0.4$ ns. This lifetime is longer than the lifetime of the $T_1 = 215$ ps we calculate using our self-consistent wave functions in Ferreira and Bastard's deformation-potential model [2] for the acoustic-phonon intersubband-scattering rate. This model does not include the modification of the acoustic phonon dispersion due to the well, and does not treat the collective-excitation nature of the intersubband excitation. We suggest that the discrepancy between theory and experiment arises from oversimplifications in the model. Band-filling effects should not play an important role as the Fermi level is 6 meV below the second subband, leaving the most important final states unoccupied.

The temperature and intensity dependence of the intersubband relaxation time was not considered in any previous experiment for $E_{1,2} < \hbar\Omega_{LO}$. Indeed, except measurements by Faist *et al.*, all have extracted T_1 from nearly saturated systems. However, the lifetime can be extracted directly from the ratio of the photovoltage [Eq. (3)] to the absorption coefficient [Eq. (2)],

$$T_1 = -\frac{P(I)}{I\alpha(I)} \frac{\hbar\omega}{e(z_{22} - z_{11})a}. \quad (4)$$

Thus, simultaneous measurements of the photovoltage and the intersubband absorption can determine T_1 over a wide range of conditions, including low intensities within the linear regime.

Thermal occupation of the excited state largely controls the temperature dependence of the intersubband absorption [solid line, Fig. 2(a)]. Figure 2(b) plots the energy relaxation rate $1/T_1$ versus $1/T$ for $T \leq 50$ K, where the measured photovoltage line shape is in good

agreement with our modeling [see Fig. 1(a)]. The quantities P and α were taken from data in Fig. 2(a). The matrix element $z_{22} - z_{11}$ was computed from our self-consistent model. As temperature increases from 10 to 50 K and the second subband becomes partially occupied, $z_{22} - z_{11}$ at -0.8 V increases only from 42 to 45 Å. In contrast, the relaxation rate increases from 8×10^8 to 1.6×10^{11} sec $^{-1}$. We fitted $1/T_1$ by the sum of two exponential functions in $1/T$, yielding activation energies of $E_A = 24 \pm 3$ meV and $E_B = 2.9 \pm 0.3$ meV. The higher activation energy probably represents the thermal barrier to relaxation by optical-phonon emission as $E_A + E_2 - E_1 \approx \hbar\Omega_{LO}$. Rosencher *et al.* observed [10] a similar, thermally activated decrease in the photovoltage signal in quantum wells, and their measurement supports our interpretation. We have no model for the weak temperature dependence of T_1 below 30 K (E_B).

For $T > 50$ K, the measured photovoltage line shape is in poor agreement with our modeling. We speculate that thermionic emission and photothermal excitation between the well and doping regions, processes not included in our model, contribute to the photovoltage and distort the line shape. Even in this regime, however, the nearly exponential dependence of the photovoltage sensitivity on inverse temperature suggests that intersubband absorption and optical-phonon emission dominate other processes.

The intersubband lifetime also depends strongly on intensity [Fig. 3(b)]. In the linear regime we measure $T_1 = 1.2$ ns, while in the strongly saturated regime ($I = 2$ kW/cm 2) we find $T_1 = 15$ ps. Craig *et al.* [7] also deduce a decrease of T_1 in a 400 Å quantum well at intensities of 1–10 W/cm 2 . We suggest two mechanisms for the reduction in lifetime at high intensities. First, the electron-electron intersubband-scattering rate is predicted to depend strongly on the population in the second subband. If this mechanism controls the relaxation, lifetime will decrease as the excited state is populated through absorption. Second, the excitation by the pump should heat the electron gas, in a way which is difficult to quantify. In view of the strong temperature dependence of the scattering rate, a reduction in the intersubband lifetime at high pump intensities is expected due to heating.

Finally, we note that the photovoltage saturates at high intensities, as the fraction of the population in the second subband asymptotically approaches $\frac{1}{2}$. In the high intensity limit, we can obtain $z_{22} - z_{11}$ directly from the photovoltage [$\Delta V = N_s^*(z_{22} - z_{11})/2$], yielding an experimental value for $z_{22} - z_{11}$ of 47 Å. This value is in excellent agreement with our simulations of an undriven quantum well at temperatures sufficient to equally populate the first and second subbands.

In summary, we have observed a photovoltage and far-infrared absorption in our coupled quantum well due to intersubband transitions. From these measurements we can extract an intersubband lifetime of 1.2 ± 0.4 ns at $T = 10$ K and low excitation intensity, substantially

longer than predicted using the formalism of Ferreira and Bastard. This appears promising for devices which can operate at low excitation and temperature, such as FIR detectors or mixers. Our results suggest that the nonradiative lifetime in a strongly excited system, such as an intersubband laser, will be much shorter, as the lifetime decreases rapidly at temperatures $T > 30$ K, and at high excitation intensities.

The authors gratefully acknowledge discussions with S.J. Allen. This work was supported by Grant No. ARO-DAAL03-92-G-0287 (J.N.H. and M.S.S.), No. ONR-N00014-92-J-1452 (J.N.H., K. Craig, and M.S.S.), the Austrian Science Foundation through the Schrödinger Fellowship (K.U.), the Alfred P. Sloan Foundation (M.S.S.), AFOSR Grant No. F49620-94-1-0158 (K. Campman, P.F.H., and A.C.G.), and the UC Regents under an INCOR grant in the area of Nonlinear Science (B.G.).

-
- [1] J. Faist, F. Capasso, D.L. Sivco, C. Sitori, A.L. Hutchinson, and A.Y. Cho, *Science* **264**, 553–556 (1994).
 - [2] R. Ferreira and G. Bastard, *Phys. Rev. B* **40**, 1074–1086 (1989).
 - [3] D.Y. Oberli, D.R. Wake, M.V. Klein, J. Klem, T. Henderson, and H. Moroc, *Phys. Rev. Lett.* **59**, 696–699 (1987).
 - [4] J.S. Levenson, G. Dolique, J.L. Oudar, and I. Abram, *Phys. Rev. B* **41**, 3688–3694 (1990).
 - [5] B.N. Murdin, G.M.H. Knippels, A.F.G. van der Meer, C.R. Pidgeon, C.J.G.M. Langerak, M. Helm, W. Heiss, K. Unterrainer, E. Gornik, K.K. Geerinck, N.J. Hovenier, and W.T. Wenckebach, *Semicond. Sci. Technol.* **9**, 1554 (1994).
 - [6] W.J. Li, B.D. McCombe, J.P. Kaminski, S.J. Allen, M.J. Stockman, L.S. Muratov, L.N. Pandey, T.F. George, and W.J. Schaff, *Semicond. Sci. Technol.* **9**, 630–633 (1994).
 - [7] K. Craig, C.L. Felix, J.N. Heyman, A.G. Markelz, M.S. Sherwin, K. Campman, P.F. Hopkins, and A.C. Gossard, *Semicond. Sci. Technol.* **9**, 627 (1994).
 - [8] J. Faist, C. Sitori, F. Capasso, L. Pfeiffer, and K. West, *Appl. Phys. Lett.* **64**, 872 (1994).
 - [9] E. Rosencher, P. Bois, E. Costard, S. Delaitre, and J. Nagle, *Appl. Phys. Lett.* **55**, 1597 (1989).
 - [10] E. Rosencher, P. Bois, B. Vinter, J. Nagle, and D. Kaplan, *Appl. Phys. Lett.* **56**, 1822–1824 (1990).
 - [11] J.N. Heyman, K. Craig, B. Galdrikian, K. Campman, P.F. Hopkins, S. Fafard, A.C. Gossard, and M.S. Sherwin, *Phys. Rev. Lett.* **72**, 2183–2186 (1994).
 - [12] J.N. Heyman, K. Craig, K. Campman, S. Fafard, A.C. Gossard, P.F. Hopkins, and M.S. Sherwin, in *Quantum Well Intersubband Transition Physics and Devices*, edited by H.C. Liu, B.F. Levine, and J.Y. Anderson (Kluwer Academic Publishers, Dordrecht, 1994), Vol. 270, pp. 467–476.
 - [13] S.J. Allen, D.C. Tsui, and B. Vinter, *Solid State Commun.* **20**, 425 (1976).